Quantification of the Interaction Forces between Metals and Graphene by Quantum Chemical Calculations and Dynamic Force Measurements under Ambient Conditions

Petr Lazar,[†,#] Shuai Zhang,[‡,#] Klára Šafářová,[†] Qiang Li,[‡] Jens Peter Froning,[†,‡] Jaroslav Granatier,[§] Pavel Hobza,[†,§] Radek Zbořil,[†] Flemming Besenbacher,[‡] Mingdong Dong,[‡,*] and Michal Otyepka[†,*]

[†]Regional Centre of Advanced Technologies and Materials, Department of Physical Chemistry, Faculty of Science, Palacký University, 771 46 Olomouc, Czech Republic, [‡]Interdisciplinary Nanoscience Center (iNANO), Aarhus University, Gustav WiedsVej 14, 8000 Aarhus C, Denmark, and [§]Institute of Organic Chemistry and Biochemistry, Academy of Sciences of the Czech Republic, Flemingovo nám. 2, 166 10 Prague 6, Czech Republic. [#]These authors contributed equally to this work.

ABSTRACT The two-dimensional material graphene has numerous potential applications in nano(opto)electronics, which inevitably involve metal graphene interfaces.Theoretical approaches have been employed to examine metal graphene interfaces, but experimental evidence is currently lacking. Here, we combine atomic force microscopy (AFM) based dynamic force measurements and density functional theory calculations to quantify the interaction between metal-coated AFM tips and graphene under ambient conditions. The results show that copper has the strongest affinity to graphene among the studied metals (Cu, Ag, Au, Pt, Si), which has important implications for the construction of a new generation of electronic devices. Observed differences in the nature of the metal—graphene bonding are well reproduced by the calculations, which included nonlocal Hartree—Fock exchange and van der Waals effects.

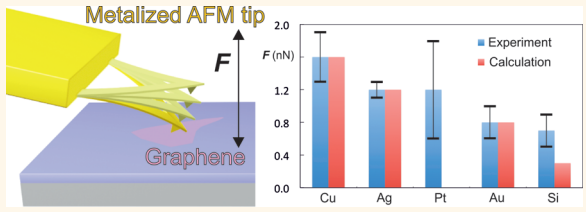

KEYWORDS: metal · graphene · interaction · nanoparticle · interaction energy · gold · platinum · copper

Graphene is a two-dimensional material with extraordinary physical properties,[1−4] making it a potentially useful material in nano(opto)electronics applications.[5−10] In this respect, most feasible applications are likely to require metal contacts linking graphene to classical electronic devices.[11,12] Furthermore, graphene has been suggested as a suitable support for metal catalysts because it is chemically inert and has a large surface area.[13−15] All the above-mentioned challenging applications call for a deeper understanding and quantification of metal binding to graphene.

The interaction of metals with graphene has been the subject of many theoretical studies,[16−19] mostly based on the density functional theory (DFT).[20,21] The nature of the interaction between metals and graphene involves many phenomena, for example, charge transfer, polarization, London dispersion forces, and relativistic effects,[22−24] which represent a challenge for theoretical calculations. In this respect, DFT calculations may provide very different results, depending on the choice of exchange-correlation (xc) functional and its ability to correctly describe the above-mentioned effects. Unfortunately, to date, experiments have been unable to identify an accurate theoretical approach. Several experimental studies have dealt with graphene/metal contacts.[13,25,26] However, so far, no experiment has quantitatively addressed the interaction force between metal and graphene. Therefore, although theoretical methods have advanced in recent years,[27−29] the development is hampered by the absence of benchmark values with which to crosscheck results and evaluate the improvement and accuracy of a particular method. There is no doubt that the experimental quantification

* Address correspondence to dong@inano.au.dk, michal.otyepka@upol.cz.

Received for review November 29, 2012 and accepted January 24, 2013.

Published online January 24, 2013
10.1021/nn305608a

of metal−graphene interactions under ambient conditions supported by suitable interaction models possesses a considerable challenge.

Here we present a combined theoretical and experimental study with the aim of quantifying the interaction between various metals and graphene. We employed advanced atomic force microscopy (AFM) to measure dynamic forces under ambient conditions and on a microsecond time scale[30−33] in order to quantify the interaction force between metalized AFM tips and graphene. The results show that Cu exhibits the highest affinity among the studied metals (Cu, Ag, Au, Pt, Si) during the adsorption and peeling processes, whereas Si exhibits the lowest. This finding has important implications with respect to the principal role of copper and silicon in current electronic devices. Moreover, the developed experimental approach is applicable for quantification of interaction forces between graphene and a large number of other metals and elements.

RESULTS AND DISCUSSION

The experiments presented in this work were conducted using sharp silicon AFM tips (Figure 1), which were coated with four different metals by thermal evaporation. The probe geometry and coating layer were characterized by scanning electron microscopy (SEM) and energy-dispersive X-ray analysis (EDS). Both the SEM images and EDS plots confirmed the homogeneous coating of all tips without any significant signs of metal oxidation (Figure 1C and Supplementary Figures 1−6). The recently developed dynamic force spectroscopy[30,31] technique involves scanning the graphene surface with a coated AFM probe (Figure 1) and measurement of the interaction force between metal and graphene as a function of time in the microsecond range. After transformation of the recorded data to force vs separation plots (Figure 2), the adhesion force was extracted, which represents the first exact quantitative information on the interaction force between metal and graphene under ambient conditions.

Figure 2A shows the morphology of a graphene single layer on a SiO_2 substrate, where the AFM experiments were carried out (for details of the experimental setup see also Figure 1A). The coated probe tapped the graphene layer with 2 kHz frequency and one force *vs* time curve was recorded per cycle. Figure 2B presents the curve obtained with a Cu-coated probe (other typical force *vs* time curves are shown in Supplementary Figure 7). Two kinds of interaction forces were recorded in one cycle; one during the approach (Figure 2B, letter B) and the other during withdrawal (Figure 2B, letter C). The interaction force during the approach (Figure 2C) corresponds to the adsorption force evaluated in our DFT calculations (Figure 3). On the other hand, the force measured

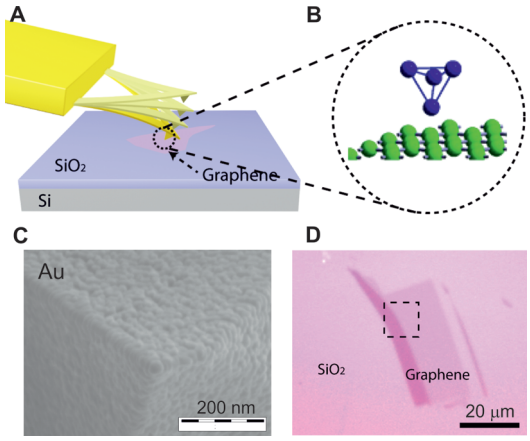

Figure 1. (A) Schematic of AFM operation in dynamic range force spectroscopy showing a metal-coated probe scanning a graphene sheet on a SiO_2 support; (B) atomic level model of metal-coated tip on graphene used in the DFT calculations; (C) SEM image of AFM tip coated by gold (see Supplementary Figure 3 for EDS spectrum); (D) optical image of the graphene substrate on SiO_2 used during the experiment. The dashed square indicates the location of the inset of Figure 2A.

during the withdrawal process (Figure 2D) corresponds to the force needed to peel graphene from the metal surface, which may also involve some surface deformation.[34−36] The calculated interaction energies and forces (E_{int}, F_{int}) and experimentally determined interaction forces (F_{app}, F_w) of different metals to graphene are summarized in Table 1 and their distributions are shown in the Supporting Information (Supplementary Figures 8 and 9). The data show unambiguously that Cu has the strongest affinity to graphene, whereas Si has the lowest. They also show that the affinity between coinage metals and graphene decreases in the order Cu > Ag > Au (Figure 4).

The calculations reveal that the strongest interaction is for the tip positioned on top of one of carbon atoms in the graphene sheet. The order of forces corresponds to the order of measured forces (the interaction is strongest for Cu, followed by Ag, and Au, and weakest for Si, see Table 1). Relativistic effects are very important in the case of Au; according to the scalar relativistic calculation (Supplementary Table 3), the Au tip has the interaction energy of 24.0 kcal/mol, and the respective force is 1.8 nN. The full relativistic calculation including spin−orbit coupling reduces the interaction force to 0.8 nN, which is in excellent agreement with the experimental data (Table 1). Figure 3 displays both the interaction energy and force curves for the Au tip over graphene calculated with various DFT functionals.

To verify our DFT results, additional calculation of the interaction of Cu, Au, Ag dimers with benzene was performed; the small size of such a model system enables a calculation with the multiconfigurational method CASPT2, which is an accurate quantum chemical method utilizing a multireference description of the many-particle wave function and second-order

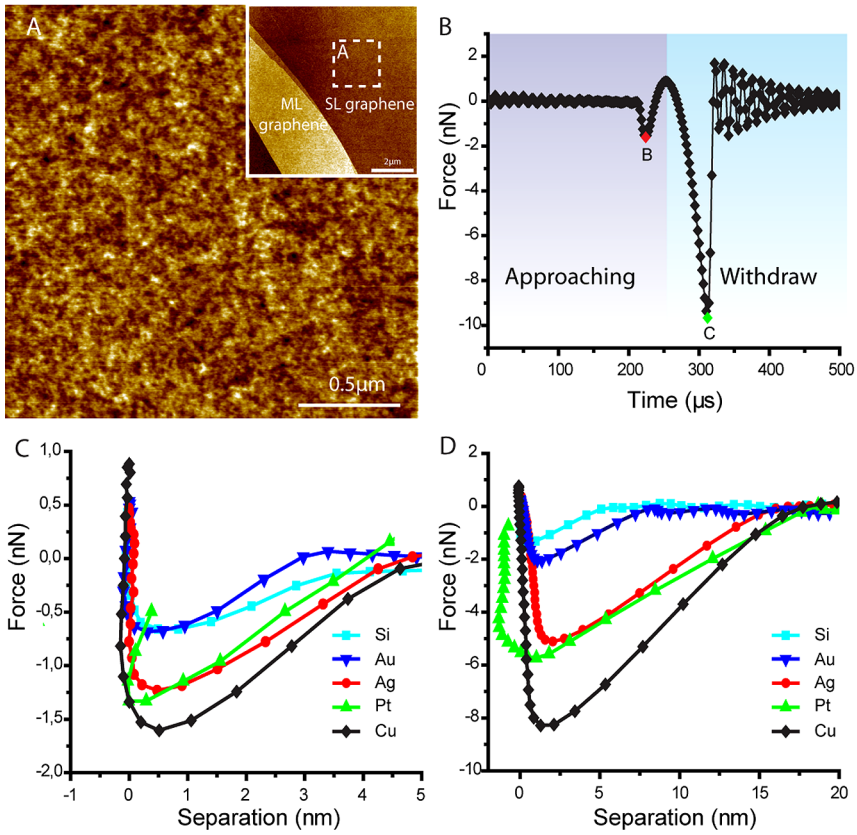

Figure 2. Graphene morphology and interaction force curves between metal-coated AFM probe and graphene: (A) AFM morphology images of graphene; (B) typical force *vs* time curve of Cu-coated probe and graphene; red B and green C dots indicate the adhesion force during approach and withdrawal, respectively; (C) typical force *vs* separation curves derived from the approach process (F_{app}); (D) typical force *vs* separation curves derived from the withdrawal process (F_w).

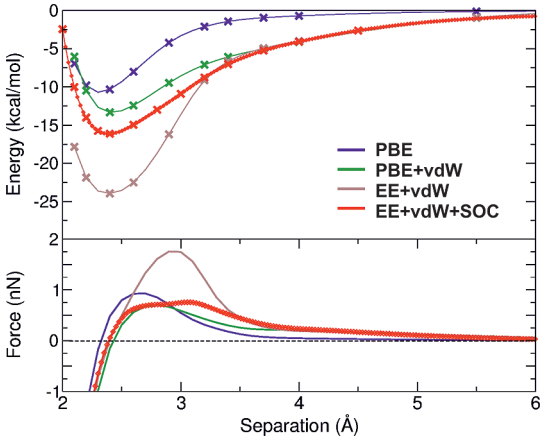

Figure 3. Calculated interaction energy curves (upper panel) and derived interaction forces (lower panel) between Au tip and graphene. The crosses denote the total energies calculated with various functionals (PBE, PBE+vdW, EE+vdW, and EE+vdW with spin−orbit coupling).

perturbation treatment of the electron correlations. The dimer axis was oriented perpendicular to the benzene ring to mimic the tip−graphene geometry. The CASPT2 results corroborated the order Cu > Au ≈ Ag of the interaction energies, confirming that the apparently strong binding of copper is not an artifact of the EE+vdW method. The different affinities of Cu, Ag, and

TABLE 1. Interaction Energies E_{int} and Forces F_{int} of a Tetrahedral Metal Tip Positioned on Top of One of Carbon Atoms of Graphene Calculated by the EE+vdW Method[a]

metal	E_{int} (kcal/mol)	F_{int} (nN)	F_{app} (nN)	F_w (nN)
Cu	24.6	1.6	1.6 ± 0.3	7.4 ± 1.4
Ag	15.8	1.3	1.2 ± 0.1	5.2 ± 0.2
Au	16.3	0.8	0.8 ± 0.2	2.0 ± 0.1
Pt	16.5		1.2 ± 0.6	6.2 ± 0.3
Si	4.9	0.3	0.7 ± 0.2	1.4 ± 0.1

[a] The experimental interaction forces were recorded during both the approach (F_{app}) and withdrawal (F_w) processes.

Au tips arise from a subtle interplay of the size effect[37] and various relativistic effects, which are crucial for the Au tip. It should be noted, that our previous study[38] showed that *planar* gold and silver tetramers are bound only by weak van der Waals interactions, which would result in lower forces. Therefore, the interaction will also depend on the geometry of the tip; a blunter geometry of the tip may decrease the measured forces.

Theoretical interaction forces agree well with the experimental data only when the EE+vdW method is used (the interaction forces calculated with various xc functionals are displayed in Table 2). The PBE functional gives consistently too low values of interaction

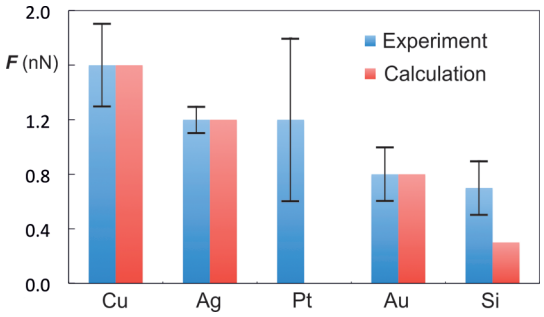

Figure 4. The experimentally derived interaction forces from the approach processes (in blue) are compared with the interaction forces calculated by the EE-vdW method (in red).

force. Its local approach to the xc energy density cannot describe long-ranged van der Waals interactions, which represent an important part of tip-support interaction. Inclusion of the nonlocal vdW correlation to the PBE functional (PBE+vdW) yields better interaction energies, but the forces are still too weak, because this functional does not reproduce well the curvature of the energy around the equilibrium distance. The combination of the vdW correlation with the exact-exchange in the EE+vdW provided accurate interaction forces. It is worth noting that this method is parameter-free and still computationally feasible, which makes it promising for further theoretical calculations of various metals on graphene support.

The order of the calculated E_{int} remained the same for other high-symmetry positions (above C−C bond, or above hollow site) on the graphene surface (Supplementary Table 1). We further calculated the interaction of the tetrahedral tips when constraining them to a singlet spin state, which may correspond to the paramagnetic state of larger metallic tip structures (Supplementary Table 2). The interaction energies for the top position (23.6, 21.2, 16.0, 25.6, and 5.0 kcal/mol for Cu, Au, Ag, Pt, and Si, respectively) indicate that the order of the metals is preserved, except for Pt. This is because Pt has the largest triplet-singlet energy difference among the studied metals, which promotes its interaction energy in the singlet state above the other metals.

The calculations also revealed interesting spin-crossover when the metals interacted with graphene; although isolated tetrahedrons of Au, Ag, and Cu have a triplet groundstate, they change into singlet spin states as they approach a graphene sheet. This triplet/singlet transition is rather abrupt and occurs when the tip apex atom approaches closer than 2.6 Å to the surface of graphene. The interaction of Pt_4 is strongly mediated by its peculiar magnetic properties; the ground-state of Pt_4 has a noncollinear arrangement of spin moments due to the spin−orbit coupling.[39] As the spin moments of Pt_4 begin to interact with graphene, several magnetic structures appear, leading to the discontinuous curve of the interaction energy. Consequently, it was not possible to extract reliable forces from the calculated data.

TABLE 2. The Interaction Force between M_4 and Graphene (F_{int} in nN) Calculated from the Numerical Derivative of the Calculated Interaction Energy (Obtained by Various Exchange-Correlation Functionals, PBE, PBE+vdW, EE+vdW, for the Preferred Position)[a]

metal	PBE	PBE+vdW	EE+vdW
Cu	1.2	0.9	1.6
Ag	0.6	0.5	1.3
Au	0.7	0.5	0.8
Au*	0.6	0.7	1.8
Si	0.02	0.2	0.3

[a] In the case of the Au_4 cluster, we also include the results calculated within a scalar relativistic approximation (denoted by an asterisk (∗)).

CONCLUSION

For the first time, we have experimentally measured the interaction force between metal and graphene using the recently developed dynamic AFM[30,31] technique by scanning the graphene surface with metal-coated AFM probes under ambient conditions. The experiments not only allowed quantification of the adhesion force but also provided information on the peeling force between various metals and graphene, which revealed that copper has both the strongest adhesion force and peeling force. Experimental results were corroborated by DFT calculations utilizing a recently introduced vdW+EE method. The order of the calculated interaction energies agreed with the order of measured forces: The interaction was strongest for Cu, followed by Au, Pt, and Ag, and weakest for Si. The interplay of size and relativistic effects can explain the different affinities of Cu, Ag, and Au tips. The calculations also revealed different mechanisms of interaction, including interesting spin-crossover in Cu, Au, and Ag clusters interacting with graphene. In general, the interaction of the graphene surface with the complex electronic structure of metal clusters exhibiting several close-lying spin states creates a subtle energy balance, which can challenge even state-of-the-art theoretical methods. In this respect, the presented experimental data have important implications for the development of theoretical methods. Moreover, the dynamic AFM technique is extremely fast and enables quantification of interaction forces with graphene for other metals that form an adequate coating on the surface of an AFM tip. From this point of view, it seems that the air atmosphere does not have the principal effect on the interaction force as the experimental data recorded in the air correlate well with DFT calculations assuming interaction in a vacuum. One possible main factor is the superhydrophobic properties of graphene, which effectively weaken

the capillary force with the coated AFM probe. The identified and quantified superior affinity of copper to graphene is very important with regard to the choice of suitable metal substrate for graphene production as well as for the construction of advanced graphene-based electronic devices.

METHODS

Preparation of Graphene Samples. The graphene sheets were deposited by mechanical exfoliation of natural graphite (Alfa Aesar) onto the silicon oxide substrate under ambient conditions. Graphene sheets were located by their contrast under optical microscopy and were further confirmed by Raman spectroscopy (data not shown) and AFM characterization.

SEM Analysis. AFM tips were characterized by scanning electron microscopy (SEM) and energy-dispersive X-ray analysis (EDS). SEM micrographs were taken on a Hitachi 6600 FEG microscope equipped with the Schottky cathode (maximum accelerating voltage of 30 kV; point-to-point resolution in secondary electrons mode (SE) 1.3 nm. Before this measurement, the sample was mounted on an aluminum holder with double-sided adhesive carbon tape. For all measurements, an accelerating voltage of 15 kV, working distance of 7 mm, and SE mode were used. EDS spectra were taken on a NORAN System 7 X-ray Microanalysis system (Thermo Scientific). For all spectra, an accelerating voltage of 15 kV, working distance of 15 mm, and lifetime of 1000 s were used. All spectra were taken from one point on the top of the AFM tips (magnification 90 000×).

AFM Method. All AFM images and force curves were recorded with Peakforce Tapping mode in a commercial Nanoscope VIII MultiMode SPM system (Bruker, Santa Barbara, CA) under ambient conditions (temperature, 24 °C; humidity, 44%). The curves were recorded using ultrasharp silicon tips (triangular, Scanasyst-Air, Bruker) with a standard spring constant of 0.4 nN/nm (the spring constant was calibrated by the Cleveland methods[40] prior to the experiment) and a normal tip radius of 2 nm. The probes were coated with various metals by vacuum evaporation. All force curves were recorded with a 2 kHz speed, and analyzed with offline software NanoScope Analysis (Bruker, Santa Barbara, CA).

Theoretical Calculations. A tetrahedral M_4 metal cluster (Figure 1B) was used as a model of an atomically sharp metalized AFM tip. Recent studies have confirmed that for atomically sharp tips, the maximum attractive force is dominated by the chemical nature of the tip apex atom and the outermost surface atom.[36,41] All tetrahedrons were positioned tip-down above a 32-atoms periodic supercell representing a graphene sheet (Figure 1B). The geometry of the metal cluster was optimized and fixed throughout the calculation of the interaction energy. The test calculation allowing geometrical relaxation of the metal cluster at an equilibrium distance to the graphene revealed only a minor change of the interaction energy (less than 5%).

The calculations were performed using the Vienna *ab Initio* Simulation Package (VASP) suite,[42,43] which makes use of the projector-augmented wave (PAW) construction for the pseudopotential. The energy cutoff for the plane-wave expansion of the eigenfunctions was set to 500 eV. The graphene sheet was modeled using a 4×4 supercell (each supercell contained 32 carbon atoms) with a calculated C−C bond length of 1.44 Å. The repeated sheets were separated from each other by 22 Å of vacuum. The shortest in-plane distance between metal atoms was 7 Å. Our test calculations have shown that the 4×4 supercell is large enough to prevent the in-plane interaction of repeated tetrahedrons. A dense $5 \times 5 \times 1$ k-point mesh was used to obtain well converged total energies, in particular in the case of exact-exchange calculation. Spin polarization was taken into account in all calculations and spin densities were allowed to relax. The interaction energies (the total energy with respect to the energies of the isolated tetrahedron and graphene sheet) were calculated using the recently developed EE+vdW method,[22] which combines a generalized gradient approximation (GGA) for the exchange functional with a van der Waals functional (vdW-DF)[44,45] and a fraction of the exact Hartree−Fock exchange. The vdW-DF adds long-range nonlocal electron−electron correlations missing in the GGA functional, and the exact exchange (EE) partly reduces the errors stemming from spurious electron self-interaction in local functionals.[46] The method has been used to obtain very accurate interaction energies of metal adatoms on graphene compared to quantum-chemical coupled-cluster calculations.[22,38] The forces were calculated from the numerical derivative of the interaction energies (interpolated by a cubic spline). Relativistic effects were included by using a scalar relativistic approximation for Cu, Ag, and Si, whereas a full relativistic description (containing spin−orbit coupling and all relativistic corrections up to order α^2, where α is the fine-structure constant) was used for Au and Pt.

Conflict of Interest: The authors declare no competing financial interest.

Acknowledgment. This work was supported by the Grant Agency of the Czech Republic [P208/12/G016]. This work was also supported by the Operational Program Research and Development for Innovations—European Regional Development Fund (CZ.1.05/2.1.00/03.0058) and European Social Fund (CZ.1.07/2.3.00/20.0017), the Danish National Research Foundation and the Villum Foundation (M.D.) and a student project of Palacký University Olomouc (PrF_2012_028). The support of Praemium Academiae of the Academy of Sciences of the Czech Republic awarded to P.H. in 2007 is also gratefully acknowledged.

Supporting Information Available: TheSupporting Information contains SEM images and EDS spectra of AFM tips (Supplementary Figures 1−6), interaction energies calculated for various positions on graphene (Supplementary Table 1) and singlet states (Supplementary Table 2) and scalar relativistic Au_4 (Supplementary Table 3), typical curves from dynamic AFM measurements (Supplementary Figure 7), and distributions of forces from AFM experiments (Supplementary Figures 8 and 9). This material is available free of charge *via* the Internet at http://pubs.acs.org.

REFERENCES AND NOTES

1. Novoselov, K. S.; Geim, A. K.; Morozov, S. V.; Jiang, D.; Zhang, Y.; Dubonos, S. V.; Grigorieva, I. V.; Firsov, A. A. Electric Field Effect in Atomically thin Carbon Films. *Science* **2004**, *306*, 666–669.
2. Novoselov, K. S.; Geim, A. K.; Morozov, S. V.; Jiang, D.; Katsnelson, M. I.; Grigorieva, I. V.; Dubonos, S. V.; Firsov, A. A. Two-Dimensional Gas of Massless Dirac Fermions in Graphene. *Nature* **2005**, *438*, 197–200.
3. Geim, A. K.; Novoselov, K. S. The Rise of Graphene. *Nat. Mater.* **2007**, *6*, 183–191.
4. Gomes, K. K.; Mar, W.; Ko, W.; Guinea, F.; Manoharan, H. C. Designer Dirac Fermions and Topological Phases in Molecular Graphene. *Nature* **2012**, *483*, 306–310.
5. Britnell, L.; Gorbachev, R. V.; Jalil, R.; Belle, B. D.; Schedin, F.; Mishchenko, A.; Georgiou, T.; Katsnelson, M. I.; Eaves, L.; Morozov, S. V.; *et al.* Field-Effect Tunneling Transistor Based on Vertical Graphene Heterostructures. *Science* **2012**, *335*, 947–950.
6. Tassin, P.; Koschny, T.; Kafesaki, M.; Soukoulis, C. M. A Comparison of Graphene, Superconductors and Metals as Conductors for Metamaterials and Plasmonics. *Nat. Photon.* **2012**, *6*, 259–264.
7. Ju, L.; Geng, B. S.; Horng, J.; Girit, C.; Martin, M.; Hao, Z.; Bechtel, H. A.; Liang, X. G.; Zettl, A.; Shen, Y. R.; *et al.* Graphene Plasmonics for Tunable Terahertz Metamaterials. *Nat. Nanotechnol.* **2011**, *6*, 630–634.

8. Kim, K.; Choi, J. Y.; Kim, T.; Cho, S. H.; Chung, H. J. A Role for Graphene in Silicon-Based Semiconductor Devices. *Nature* **2011**, *479*, 338–344.
9. Bunch, J. S.; van der Zande, A. M.; Verbridge, S. S.; Frank, I. W.; Tanenbaum, D. M.; Parpia, J. M.; Craighead, H. G.; McEuen, P. L. Electromechanical Resonators from Graphene Sheets. *Science* **2007**, *315*, 490–493.
10. Kim, K. S.; Zhao, Y.; Jang, H.; Lee, S. Y.; Kim, J. M.; Kim, K. S.; Ahn, J.-H.; Kim, P.; Choi, J.-Y.; Hong, B. H. Large-Scale Pattern Growth of Graphene Films for Stretchable Transparent Electrodes. *Nature* **2009**, *457*, 706–710.
11. Leonard, F.; Talin, A. A. Electrical Contacts to One- and Two-Dimensional Nanomaterials. *Nat. Nanotechnol.* **2011**, *6*, 773–783.
12. Lee, H.; Heo, K.; Park, J.; Park, Y.; Noh, S.; Kim, K. S.; Lee, C.; Hong, B. H.; Jian, J.; Hong, S. Graphene-nanowire Hybrid Structures for High-Performance Photoconductive Devices. *J.Mater. Chem.* **2012**, *22*, 8372–8376.
13. Zan, R.; Bangert, U.; Ramasse, Q.; Novoselov, K. S. Interaction of Metals with Suspended Graphene Observed by Transmission Electron Microscopy. *J. Phys. Chem. Lett.* **2012**, *3*, 953–958.
14. Georgakilas, V.; Otyepka, M.; Bourlinos, A. B.; Chandra, V.; Kim, N.; Kemp, K. C.; Hobza, P.; Zboril, R.; Kim, K. S. Functionalization of Graphene: Covalent and Noncovalent Approaches, Derivatives and Applications. *Chem. Rev.* **2012**, *112*, 6156–6214.
15. Myung, S.; Yin, P. T.; Kim, C.; Park, J.; Solanki, A.; Reyes, P. I.; Lu, Y. C.; Kim, K. S.; Lee, K. B. Label-free Polypeptide-Based Enzyme Detection Using a Graphene-Nanoparticle Hybrid Sensor. *Adv. Mater.* **2012**, *24*, 6081–6087.
16. Chan, K. T.; Neaton, J. B.; Cohen, M. L. First-Principles Study of Metal Adatom Adsorption on Graphene. *Phys. Rev. B* **2008**, *77*, 235430.
17. Giovannetti, G.; Khomyakov, P. A.; Brocks, G.; Karpan, V. M.; van den Brink, J.; Kelly, P. J. Doping Graphene with Metal Contacts. *Phys. Rev. Lett.* **2008**, *101*, 026803.
18. Johll, H.; Kang, H. C.; Tok, E. S. Density Functional Theory Study of Fe, Co, and Ni Adatoms and Dimers Adsorbed on Graphene. *Phys. Rev. B* **2009**, *79*, 245416.
19. Khomyakov, P. A.; Giovannetti, G.; Rusu, P. C.; Brocks, G.; van den Brink, J.; Kelly, P. J. First-Principles Study of the Interaction and Charge Transfer between Graphene and Metals. *Phys. Rev. B* **2009**, *79*, 195425.
20. Hohenberg, P.; Kohn, W. Inhomogeneous Electron Gas. *Phys. Rev. B* **1964**, *136*, B864.
21. Kohn, W.; Sham, L. J. Self-Consistent Equations Including Exchange and Correlation Effects. *Phys. Rev.* **1965**, *140*, 1133.
22. Granatier, J.; Lazar, P.; Otyepka, M.; Hobza, P. The Nature of the Binding of Au, Ag, and Pd to Benzene, Coronene, and Graphene: From Benchmark CCSD(T) Calculations to Plane-Wave DFT Calculations. *J. Chem. Theory Comput.* **2011**, *7*, 3743–3755.
23. Vanin, M.; Mortensen, J. J.; Kelkkanen, A. K.; Garcia-Lastra, J. M.; Thygesen, K. S.; Jacobsen, K. W. Graphene on Metals: A van der Waals Density Functional Study. *Phys. Rev. B* **2010**, *81*, 081408.
24. Olsen, T.; Yan, J.; Mortensen, J. J.; Thygesen, K. S. Dispersive and Covalent Interactions between Graphene and Metal Surfaces from the Random Phase Approximation. *Phys. Rev. Lett.* **2011**, *107*, 156401.
25. Venugopal, A.; Colombo, L.; Vogel, E. M. Contact Resistance in Few and Multilayer Graphene Devices. *Appl. Phys. Lett.* **2010**, *96*, 013512.
26. Pi, K.; McCreary, K. M.; Bao, W.; Han, W.; Chiang, Y. F.; Li, Y.; Tsai, S. W.; Lau, C. N.; Kawakami, R. K. Electronic Doping and Scattering by Transition Metals on Graphene. *Phys. Rev. B* **2009**, *80*, 075406.
27. Schimka, L.; Harl, J.; Stroppa, A.; Gruneis, A.; Marsman, M.; Mittendorfer, F.; Kresse, G. Accurate Surface and Adsorption Energies from Many-Body Perturbation Theory. *Nat. Mater.* **2010**, *9*, 741–744.
28. Grimme, S. Density Functional Theory with London Dispersion Corrections. *WIREs Comput. Mol. Sci.* **2011**, *1*, 211–228.
29. Cramer, C. J.; Truhlar, D. G. Density Functional Theory for Transition Metals and Transition Metal Chemistry. *Phys. Chem. Chem. Phys.* **2009**, *11*, 10757–10816.
30. Dong, M.; Sahin, O. A Nanomechanical Interface to Rapid Single-Molecule Interactions. *Nat. Commun.* **2011**, *2*, 247.
31. Dong, M. D.; Husale, S.; Sahin, O. Determination of Protein Structural Flexibility by Microsecond Force Spectroscopy. *Nat. Nanotechnol.* **2009**, *4*, 514–517.
32. Rico, F.; Su, C.; Scheuring, S. Mechanical Mapping of Single Membrane Proteins at Submolecular Resolution. *Nano Lett.* **2011**, *11*, 3983–3986.
33. Medalsy, I.; Hensen, U.; Muller, D. J. Imaging and Quantifying Chemical and Physical Properties of Native Proteins at Molecular Resolution by Force-Volume AFM. *Angew. Chem., Int. Ed.* **2011**, *50*, 12103–12108.
34. Lantz, M. A.; Hug, H. J.; Hoffmann, R.; van Schendel, P. J. A.; Kappenberger, P.; Martin, S.; Baratoff, A.; Guntherodt, H. J. Quantitative Measurement of Short-Range Chemical Bonding Forces. *Science* **2001**, *291*, 2580–2583.
35. Hoffmann, R.; Kantorovich, L. N.; Baratoff, A.; Hug, H. J.; Guntherodt, H. J. Sublattice Identification in Scanning Force Microscopy on Alkali Halide Surfaces. *Phys. Rev. Lett.* **2004**, *92*, 146103.
36. Sugimoto, Y.; Pou, P.; Abe, M.; Jelinek, P.; Perez, R.; Morita, S.; Custance, O. Chemical Identification of Individual Surface Atoms by Atomic Force Microscopy. *Nature* **2007**, *446*, 64–67.
37. Yi, H.-B.; Diefenbach, M.; Choi, Y. C.; Lee, E. C.; Lee, H. M.; Hong, B. H.; Kim, K. S. Interactions of Neutral and Cationic Transition Metals with the Redox System of Hydroquinone and Quinone: Theoretical Characterization of the Binding Topologies, and Implications for the Formation of Nanomaterials. *Chem.—Eur. J.* **2006**, *12*, 4885–4892.
38. Granatier, J.; Lazar, P.; Prucek, R.; Safarova, K.; Zboril, R.; Otyepka, M.; Hobza, P. Interaction of Graphene and Arenes with Noble Metals. *J. Phys. Chem. C* **2012**, *116*, 14151–14162.
39. Blonski, P.; Dennler, S.; Hafner, J. Strong Spin-orbit Effects in Small Pt Clusters: Geometric Structure, Magnetic Isomers and Anisotropy. *J. Chem. Phys.* **2011**, *134*, 034107.
40. Cleveland, J. P.; Manne, S.; Bocek, D.; Hansma, P. K. A Nondestructive Method for Determining the Spring Constant of Cantilevers for Scanning Force Microscopy. *Rew. Sci. Instrum.* **1993**, *64*, 403–405.
41. Pou, P.; Ghasemi, S. A.; Jelinek, P.; Lenosky, T.; Goedecker, S.; Perez, R. Structure and Stability of Semiconductor Tip Apexes for Atomic Force Microscopy. *Nanotechnology* **2009**, *20*, 264015.
42. Blochl, P. E. Projector Augmented-Wave Method. *Phys. Rev. B* **1994**, *50*, 17953–17979.
43. Kresse, G.; Joubert, D. From Ultrasoft Pseudopotentials to the Projector Augmented-Wave Method. *Phys. Rev. B* **1999**, *59*, 1758–1775.
44. Dion, M.; Rydberg, H.; Schroder, E.; Langreth, D. C.; Lundqvist, B. I. Van der Waals Density Functional for General Geometries. *Phys. Rev. Lett.* **2004**, *92*, 246401.
45. Klimes, J.; Bowler, D. R.; Michaelides, A. Van der Waals Density Functionals Applied to Solids. *Phys. Rev. B* **2011**, *83*, 195313.
46. Cohen, A. J.; Mori-Sanchez, P.; Yang, W. T. Challenges for Density Functional Theory. *Chem. Rev.* **2012**, *112*, 289–320.